PHYSICAL REVIEW D **86,** 114034 (2012)

Charged Z' to conciliate the apparent disagreement between $t\bar{t}$ Tevatron forward-backward asymmetry and LHC charge asymmetry

Ezequiel Álvarez[1,2,*] and Estefania Coluccio Leskow[1,†]

[1]*CONICET, IFIBA, Departamento de Física, FCEyN, Universidad de Buenos Aires, Ciudad Universitaria, Pabellon 1, 1428 Ciudad de Buenos Aires, Argentina*

[2]*CONICET, INFAP, Departamento de Física, FCFMyN, Universidad Nacional de San Luis, Avenida Ejército de los Andes 950, 5700 San Luis, Argentina*

(Received 27 September 2012; published 21 December 2012)

We propose a charged, electrically neutral, and flavor-changing Z' model to conciliate the apparent disagreement between the important excess found in the $t\bar{t}$ Tevatron forward-backward asymmetry and the null—compatible with negative—results found in the LHC charge asymmetry. We show that this model contributes positively to the forward-backward asymmetry, whereas naturally a new cancellation is turned on at the LHC, yielding a null, or even negative, charge asymmetry. We find the region in parameter space that is simultaneously allowed by the stringent Tevatron and LHC observables. We show that the model is safe to atomic parity violation constraints and propose a possible increase in the Z' width to avoid restrictions coming from $tj/\bar{t}j$ resonance searches and $t\bar{t}j$ cross section. We evaluate the constraints to the model, as well as distinctive features in the forecoming experimental results.

DOI: 10.1103/PhysRevD.86.114034 PACS numbers: 14.65.Ha

I. INTRODUCTION

The recent discovery of a new Higgs-like boson by the ATLAS [1] and CMS [2] Collaborations at the LHC, with a mass of approximately 125 GeV, is an exceptional step towards the verification of the Standard Model (SM). The SM has been tested by many experiments over the past decades and has successfully described high-energy particle interactions. However, the electroweak symmetry breaking mechanism has not been yet understood. The LHC will be extensively devoted to this subject and to measuring the properties of the new particle in order to explore the underlying theory from which it arises. The understanding of this new particle interaction could be an important probe of new physics (NP) in coming years.

Another particle sensitive to NP is the top quark [3], not only because its mass is close to the electroweak symmetry breaking scale but also because of its relatively little exploration. Experimental results that could give us hints of NP effects in this sector have been reported [4,5], being the $p\bar{p} \to t\bar{t}$ forward-backward asymmetry (A_{FB}) measurement, probably one of the most remarkable ones. Both the CDF and D0 Collaborations measured the $t\bar{t}$ cross section ($\sigma_{t\bar{t}}$) in good agreement with the SM [6]; however, there exists a discrepancy in the A_{FB} between the theory and the experimental results. This asymmetry enables the study of the top pair production mechanism, and it is customary to define it as

$$A_{FB} = \frac{N(\Delta y > 0) - N(\Delta y < 0)}{N(\Delta y > 0) + N(\Delta y < 0)}, \tag{1}$$

where $\Delta y = y_t - y_{\bar{t}}$ is the difference in rapidity of top and antitop quarks along the proton momentum direction.

While the SM prediction for A_{FB} at next-to-leading order (NLO) in QCD is 0.087 ± 0.01 [7], results from CDF and D0 report excesses in their measured asymmetries already from the first published results [8] in 2008. The most recent CDF results give an inclusive parton level asymmetry of $A_{FB} = 0.162 \pm 0.047$ [9] in agreement with an independent D0 measurement of $A_{FB} = 0.196 \pm 0.065$ [10]. The largest disagreement with the SM A_{FB} prediction was announced this year by CDF in the differential measurements for $A_{FB}(M_{t\bar{t}})$ and $A_{FB}(|y_t - y_{\bar{t}}|)$ [9]. The fitted results of these differential measurements have a p-value statistical significance of $p = 0.006$ and $p = 0.008$, respectively.

Many NP models [11] arose to account for the excess measured in the A_{FB}. If this excess is generated by new physics, then these models could be tested at the LHC. Since this machine is a symmetric pp collider, the top quark forward-backward asymmetry vanishes. However, an asymmetry in charge (A_C) can be measured, and it is defined by

$$A_C = \frac{N(\Delta|y| > 0) - N(\Delta|y| < 0)}{N(\Delta|y| > 0) + N(\Delta|y| < 0)}. \tag{2}$$

The current experimental values for A_C are $A_C = 0.029 \pm 0.018 \pm 0.014$ at ATLAS [12] and $A_C = 0.004 \pm 0.010 \pm 0.011$ at CMS [13], both consistent with the SM prediction of 0.0115 ± 0.0006 [7]. Almost all the models that tried to explain the large A_{FB} also predicted a large value for A_C, and as a result most of them were excluded.

According to the nature of the new particle exchange, these models fall mainly into two sets: those with new s-channel processes and those with a new t-channel

*sequi@df.uba.ar
†ecoluccio@df.uba.ar

exchange mediator. Many of these models have already been discarded not only due to A_{FB} and A_C but also to other precision LHC measurements. For instance, dijet observables [14,15] have excluded many s-channel models, while t-channel ones such as flavor-changing neutral current Z' models [16–19] have been discarded by same-sign top pair production [20,21]. In order to avoid this last constraint, models with a charged Z' and/or a W'[1] arose [22–25]. An example of this kind of model is a specific one [26] where a horizontal gauge symmetry yields a flavor-changing and a flavor-conserving neutral boson which has been discarded by atomic parity violation (APV) observables [24].

In this paper [27], we study a phenomenological charged Z' model with flavor-violating couplings to u and t quarks. We stress that the new boson is electrically neutral. This Z' has a mass larger than the top mass and no other partner coming from gauge invariance [24,26]. The reasons for this phenomenological model come out to be twofold: (i) constraints as flavor-changing neutral current top decays and same-sign top production are avoided, whereas APV constraints are largely relaxed; and (ii) it appears a cancellation in A_C which is not present in A_{FB}, yielding a possible explanation for the apparent disagreement between these observables.

This model could solve the apparent disagreement between A_{FB} and A_C in an innovative way. In most of the models that try to account for the large A_{FB} measured at the Tevatron, the excess in this asymmetry also implies an excess in A_C, and the agreement is sought as an intermediate balance in which A_C is not too large while A_{FB} is not too small. In the model presented in this paper, on the other hand, the agreement in some part of the parameter space has to be sought as making A_{FB} large without making A_C too negative.

We study the Tevatron and LHC phenomenology of this model and verify that the cancellation takes place, making possible the simultaneous explanation not only of both A_{FB} and A_C, but also of all CDF unfolded results, APV, and LHC $t\bar{t}$ cross section within the 95% C.L. However, the model is sensitive to $tj/\bar{t}j$ resonance searches and also predicts an excess in the $t\bar{t}j$ final state. To avoid this difficulty, we explore the possibility of increasing the Z' width, assuming that the Z' decays to not-detectable particles a fraction of the times. Although it is not the purpose of this paper to address the fate of the invisible decay, we mention that these particles could be, for instance, dark matter or sterile neutrinos. This new feature of the model predicts single-top production with a particular topology, which we also explore.

This paper is divided as follows. In the next section, we present the model and its phenomenology and explain how the cancellation in A_C takes place at the LHC. In Sec. III, we perform Monte Carlo simulations of the Tevatron and LHC, and we find the region in parameter space compatible with all the constraints. In Sec. IV, we discuss constraints and predictions for the model, and Sec. V contains the conclusions.

[1]Throughout this paper, Z' refers to an *electrically neutral* boson and W' to an electrically charged one.

II. PHENOMENOLOGY OF A CHARGED Z' MODEL

In this section we present the Lagrangian of a phenomenological Z' model together with a description of its contributions to the $t\bar{t}$ forward-backward asymmetry at the Tevatron and charge asymmetry at the LHC. We find the expected constraints to the model, which are analyzed in Sec. IV.

A. The model

We consider a model containing a charged, spin-one, colorless particle with flavor-violating interactions which we call Z'. We assume this particle couples only to right-handed u and t quarks, since the left-handed coupling is constrained by B physics [28,29]. We also assume that its mass is larger than the top mass, avoiding a flavor-changing top decay [30]. The interacting part of the phenomenological NP Lagrangian is then given by

$$\mathcal{L}_{\mathrm{NP}} = f_R \bar{u}\gamma^\mu P_R t Z'_\mu + f_R \bar{t}\gamma^\mu P_R u Z'^\dagger_\mu, \tag{3}$$

where $P_R = \frac{(1+\gamma^5)}{2}$ and f_R is the right-handed coupling.

It is important to note that we are considering a charged boson, so that Z'_μ is not the same particle as its conjugate partner $Z'^\dagger_\mu$. Under this condition, the production of same-sign tops is forbidden. Models in which these two particles are the same particle, i.e., models with *neutral* Z' bosons, allow the production of same-sign top pairs and, as a consequence, are excluded [31].

B. Phenomenology for Tevatron and LHC $t\bar{t}$ asymmetries

The Feynman diagrams for pp, $p\bar{p} \to t\bar{t}(u)$ involving a Z' boson in the model described previously are shown in Fig. 1. We denote by t_1 the diagram where this particle is exchanged through a t channel and by s_1 and s_2 those diagrams where the Z' goes through an s channel. In the former case, the Z' contributes to a $t\bar{t}$ final state, while in the latter to $t\bar{t}u$ production. Since $Z' \neq Z'^\dagger$, s_1 and s_2 have different conjugate diagrams, $\bar{s}_1$ and $\bar{s}_2$, which at the Tevatron, due to the symmetry in $p \leftrightarrow \bar{p}$, have the same strength as s_1 and s_2. On the contrary, at the LHC, $\sigma(\bar{s}_1, \bar{s}_2) \ll \sigma(s_1, s_2)$.

The cornerstone of our analysis is the observation that at the LHC there is a cancellation of the charge asymmetry coming from the contributions of the t- and s-channel processes, explaining the small and compatible with negative charge asymmetry measured by this experiment. This cancellation is not present at the Tevatron, where as a

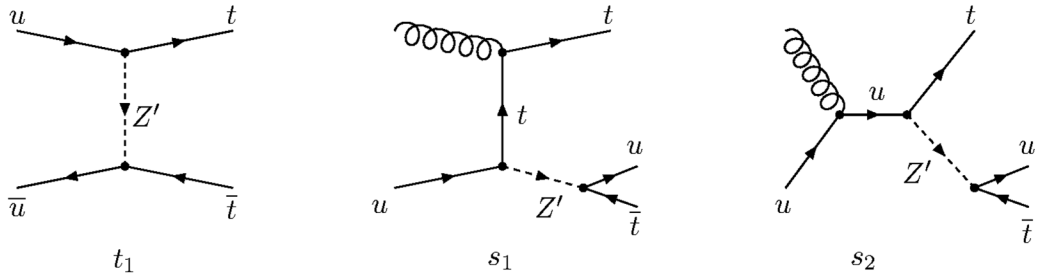

FIG. 1. Feynman diagrams for pp, $p\bar{p} \to t\bar{t}(u)$ involving a Z': In t_1 the Z' is exchanged through a t channel, and in s_1 and s_2 the Z' goes through an s channel. We show that s_1 cancels the contribution to the charge asymmetry of t_1 at the LHC.

matter of fact a large A_{FB} has been measured. We see in the following paragraphs how the t-channel diagram contributes positively to the asymmetries, while at the LHC the s-channel ones have a negative contribution.

To understand this cancellation, it is important to clarify two points. First is the reason why the t channel contributes positively to both the A_C and the A_{FB} asymmetries whereas the s-channel contribution is negative and only noticeable at the LHC. Second is why the t-channel process is privileged at the Tevatron while the s channel is turned on at the LHC.

To study the first point, one should first realize that the s_2 process is suppressed with respect to s_1 and t_1, since the up quark propagator carries all the energy of the process. We can then compare t_1 and s_1 (which is a t-channel diagram if thought up to the tZ' final state) by studying the general dynamics of a t-channel process.

In a general t-channel 1, $2 \to 1''$, 2 process, where the same number indicates a shared vertex, the relevant factor coming from the propagator of an exchanged X particle is

$$\frac{1}{(p_1 - p_{1'})^2 - m_X^2} = \frac{1}{m_1^2 + m_{1'}^2 - 2E_1E_{1'} + 2\vec{p}_1.\vec{p}_{1'} - m_X^2}. \tag{4}$$

In general, m_1 can be neglected. For the case $m_{1'} < m_X$ (t_1 in Fig. 1), the events with the largest cross sections are those where $\vec{p}_1.\vec{p}_{1'} > 0$. For the sake of brevity, we refer to this condition as 1 and 1' having the same direction and to $\vec{p}_1.\vec{p}_{1'} < 0$ as having opposite direction. If $m_{1'} > m_X$ (s_1 in Fig. 1), the same holds unless E_1 is too small, although it can be seen in the center of mass system that this is kinetically forbidden for this specific process. Note that, although there will also be contributions coming from the Lorentz structure of the vertices, the only analysis of the dynamic in Eq. (4) already results in a good approach to compare diagrams t_1 and s_1.

From this reasoning we see that, in the t-channel diagram t_1 of Fig. 1, the top quark is likely to have the same direction as the incoming up quark, contributing to a *positive* asymmetry.

Following the same logic, in the s-channel diagram s_1 of Fig. 1, the Z' boson is the one that tends to have the same direction as the incoming up quark and transmits it to its decay products $\bar{t}$ and u. This results in a *negative* contribution to the asymmetry. At this point, it is interesting to note that at the Tevatron s_1 and its conjugate contribute the same; however, at the LHC s_1 dominates over $\bar{s}_1$, and as a result the net contribution from these two diagrams to the charge asymmetry is negative and that is why the s channel effectively contributes to the asymmetry only in this experiment.

The second point to analyze involves two questions: why the s channel is turned on at the LHC and why the t-channel process dominates at the Tevatron. The first one has to do with the energy of the accelerator: Since at the LHC the phase space is larger than at the Tevatron, the s channel, which has a Z' on shell, is turned on in this machine resulting in a cancellation of the charge asymmetry when all the processes are considered. The second one concerns the nature of the collisions at the Tevatron: The t-channel process is privileged, because it involves antiquarks, present in the colliding antiprotons, so its positive contribution is enhanced in the forward-backward asymmetry measured in this accelerator.

In summary, let us remark once again that the s channel, having a negative contribution to the asymmetry, is crucial for the cancellation of the charge asymmetry and thus for the simultaneous explanation of the forward-backward and charge asymmetry measurements.

C. Expected constraints to the model

We refer in this subsection to the expected constraints to the model in a qualitative way. We study all of them in some depth in Secs. III and IV.

A direct constraint to the model comes from $tj/\bar{t}j$ resonance searches. Apart from our model, many other models of NP [32–34] predict a resonance in the $tj/\bar{t}j$ system of $t\bar{t}j$ final state. We analyze in Sec. IV the experimental constraints coming from these resonance searches and propose new decays for the Z' such as dark matter or sterile neutrinos in order to avoid this limit. These new decays imply an increment of the Z' width which affects only the s-channel processes; the t_1 process is not altered since the f_R coupling remains the same and Z' is not on shell

in this channel. Moreover, in this way one of the indirect constraints to the model, which is the limit in $t\bar{t}j$ production, also gets relaxed because of the width increase.

Observe that the increment of the Z' width caused by the new invisible decays of this particle results in a particular single-top production topology. In fact, when the Z' decays to undetectable particles, the final state will be a top, missing energy, and with no b jets.

Another indirect constraint comes from APV. The $Z'tu$ vertex generates one-loop corrections to the Zuu effective coupling that affect low-energy precision tests of parity-violating observables [24,35]. The strongest constraints come from APV measurements in cesium [36]. We investigate the parity-violating atomic transitions sensitive to the nuclear weak charge within this model and show the results in Secs. III and IV.

III. NUMERICAL RESULTS

The analysis of the previous section led us to the understanding of the charge asymmetry cancellation mechanism, which makes possible the simultaneous explanation of the forward-backward and charge asymmetry experimental results at the Tevatron and the LHC, respectively. In this section, we search numerically for this cancellation and investigate the allowed parameter space of the model by confronting it with many relevant observables and with the major constraints discussed in the previous section. The parameter space considered is delimited by 200 GeV $< M_{Z'} <$ 500 GeV and $0.5 < f_R < 1.2$.

Using MADGRAPH5 [37] with the default tuning, including variable factorization and renormalization scales, we simulate $t\bar{t}(u)$ production at the Tevatron and the LHC at 7 TeV within the Z' model at parton level according to the diagrams of Fig. 1 and their conjugates, in addition to the SM LO $t\bar{t}$ contribution. Since in the SM these processes do not generate a charge asymmetry, the A_C computed with the simulated collisions contains NP contributions only. Hence, in order to compute the model predictions, it is necessary to include the SM at NLO contribution to A_C.

If the NP contribution to the total cross section is small, $\sigma_{\mathrm{SM}} \gg \sigma_{\mathrm{NP}}$ (where σ_{NP} contains both SM-NP interference and NP squared contributions), we can approximate the asymmetry by [38]

$$A_C \approx A_C^{\mathrm{NP+SM@LO}} + A_C^{\mathrm{SM@NLO}}. \tag{5}$$

We study the Z' model in the parameter space previously mentioned confronting it with the last differential measurements of A_{FB} [9] and $\sigma_{t\bar{t}}$ [39] at the parton level from CDF and $\sigma_{t\bar{t}}$ [40] and A_C [13] from CMS. We use CDF results since their discrepancy with the SM has larger statistical significance than those of D0 [10], and the main purpose of this work is to present a model capable of reconciling two measurements (A_{FB} and A_C) which may seem to be in disagreement. On the other hand, we use CMS measurements because they yield the most precise results. We perform a χ^2 test with all the observables measured at CDF and confront the model with all the other ones in a separate way each. We analyze each of these constraints in the following paragraphs.

The last measurement of A_{FB} published by CDF [9] shows A_{FB} as a function of both the invariant mass $M_{t\bar{t}}$ and Δy. The ranges for the bins used in that analysis, and in our χ^2 test, are $[0-450; 450-550; 550-650; 650-\infty]$ GeV for $M_{t\bar{t}}$ and $[0-0.5; 0.5-1; 1-1.5; 1.5-\infty]$ for Δy. By requiring the p value to be greater than 0.05, we select the points in parameter space which are in agreement with CDF results at a 95% C.L. The $M_{Z'}$ vs f_R region consistent with Tevatron measurements is delimited by the green dashed lines present in all the figures that follow in this section.

To confront our model against the measurement of the inclusive $t\bar{t}$ cross section at the LHC, we do as follows. We take as the experimental input for the inclusive LHC at 7 TeV $t\bar{t}$ cross section the CMS combination, which is 165.8 ± 13.3 pb [40]; whereas for the theoretical input we use the calculation made with HATHOR, which gives 164^{+11}_{-16} pb [41]. Since their central values agree, and their errors summed in quadrature represent a 13% of the cross section, we test the cross section in the simulations of our model against a similar simulation with only the SM and we set the error to be the 13% of the cross section. It can be shown that this procedure is equivalent to using a K factor. Since our NP final state goes up to $t\bar{t}j$, we do the SM corresponding simulation and use PYTHIA to account for initial and final state radiation and the MLM (Mangano) matching scheme [42] to avoid double counting.

We first analyze, separately, the positive and negative contributions to the charge asymmetry discussed in the previous section with the only purpose of explicitly observing each of them.

We define the t- and s-channel charge asymmetries, A_{C_t} and A_{C_s},

$$A_{C_t} = \frac{N^+(t,\mathrm{SM}) - N^-(t,\mathrm{SM})}{N^+(t,\mathrm{SM}) + N^-(t,\mathrm{SM}) + N^+(s) + N^-(s)}, \tag{6}$$

$$A_{C_s} = \frac{N^+(s) - N^-(s)}{N^+(t,\mathrm{SM}) + N^-(t,\mathrm{SM}) + N^+(s) + N^-(s)}, \tag{7}$$

where $N^{+(-)}(t,\mathrm{SM})$ is the number of events with a positive (negative) value of $\Delta|y|$ when the t-channel and the SM processes at tree level are considered, while $N^{+(-)}(s)$ denotes the same quantity except that in this case only the s-channel processes are taken into account. With these definitions the charge asymmetry of NP + SM@LO is given by

$$A_C^{\mathrm{NP+SM@LO}} = A_{C_t} + A_{C_s}. \tag{8}$$

We show in Figs. 2 and 3 the t- and s-channel contributions to the charge asymmetry, respectively. For an easier visualization, the background colors in the plots indicate

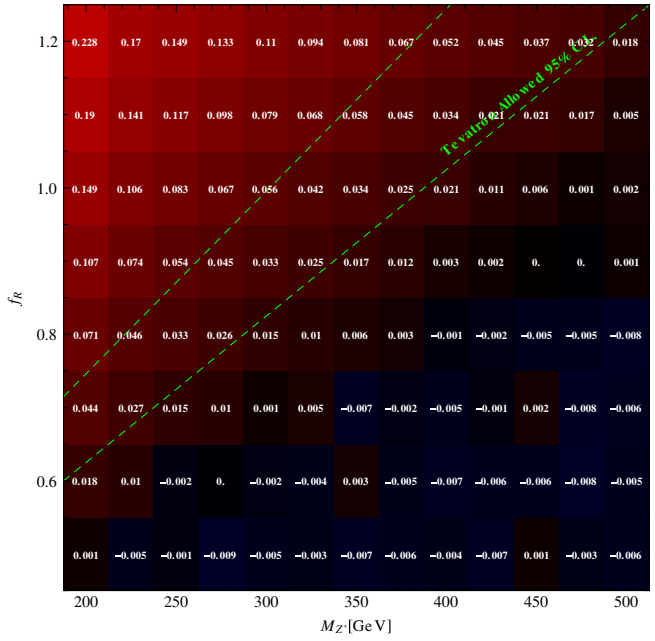

FIG. 2 (color online). t-channel contribution to the charge asymmetry as a function of $M_{Z'}$ and f_R. If this contribution would be the only NP contribution to A_C, then it should be below 0.023 in order to be consistent at a 95% C.L. with the experimental data [13] and the theory prediction [7]. In order to visualize patterns, we plotted in red (blue) the positive (negative) contributions. The tone of the color stands for the absolute value of the contribution. As predicted, there is a predominance of positive contributions which is usually above the 95% C.L. allowance.

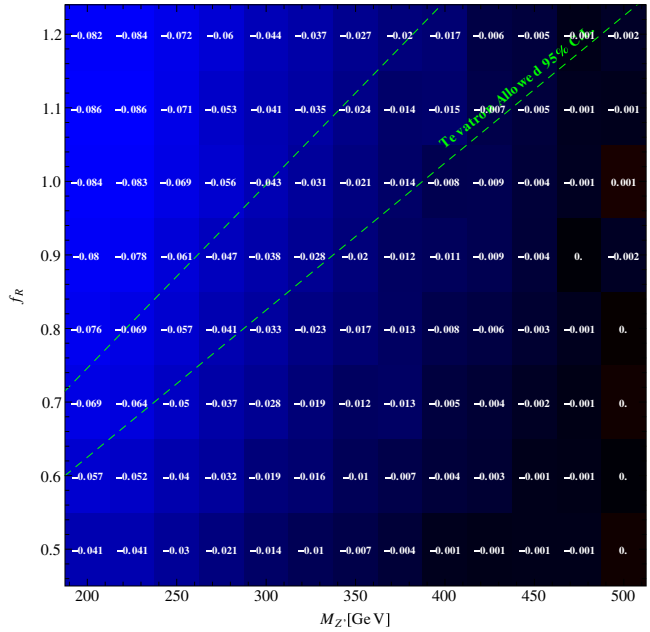

FIG. 3 (color online). The same as the previous figure but for the s-channel contribution to the charge asymmetry. If this contribution would be the only NP contribution to A_C, then it should be above -0.037 in order to be consistent at a 95% C.L. with the experimental data [13] and the theory prediction [7].

the sign of the contribution for every point in the parameter space; red (blue) represents a positive (negative) sign. The tone of the colors stands for the absolute value of the contribution; the more intense the tone, the larger the absolute value. Note that these plots clearly exhibit the cancellation of the charge asymmetry in the region defined by Tevatron limits. In Fig. 2 the NP contribution is mainly positive while in Fig. 3 is mainly negative, which results in the expected cancellation of the charge asymmetry discussed in the previous section.

We show in Fig. 4 the contributions of both A_{C_t} and A_{C_s} using the same convention of colors and tones as in the two previous figures with the distinction that now in every cell there are two numbers. The new number below is the difference of the model prediction for the $t\bar{t}$ inclusive cross section to the measured value, in units of the error, as previously explained. The area delimited by the triangle contains the region consistent with Tevatron limits in which these two observables differ by less than 2 from their corresponding experimental values in units of the experimental error. The dot-dashed lines limit the region excluded by $tj/\bar{t}j$ resonance searches by CDF, while the region above the solid line corresponds to the same searches by ATLAS. To avoid this last constraint, we propose an increase in the Z' width which is discussed below. The parameter space above the thick dotted line shows the APV excluded region. We discuss these constraints in the next section.

The results in Fig. 4 show that the Z' width should be increased to avoid constraints coming from $tj/\bar{t}j$ resonance searches. This increase would also be required to avoid possible limits coming from the $t\bar{t}j$ production cross section. Since there are not available works on $t\bar{t}j$ limits that could be adapted to our model, we use in the next section $W'td$ production results from Ref. [43] as a rough estimation of the $t\bar{t}j$ production at the LHC in our model. We repeated the simulations for values of the Z' width increased by three different factors and searched again for the allowed parameter space in these cases. We show in Fig. 5 the allowed region for a Z' width 3 (orange dotted line), 5 (blue dot-dashed line), and 7 (magenta dashed line) times its value when the decay is solely to u and $\bar{t}$, which we denote by Γ_0. We also show in this plot the yellow (solid) triangle of Fig. 4 that corresponds to no change in the Z' width. We checked that the narrow width approximation holds for all the values of the Z' width considered.

The first remark concerning Fig. 5 is that, as can be seen, Tevatron results are not affected by the Z' width modification. The second one has to do with the width increment effect on the allowed parameter space. Let us now analyze this point and start by investigating why the allowed region defined by the yellow (solid) triangle in Fig. 4 (also shown in Fig. 5) gets excluded when larger values of the Z' width are considered.

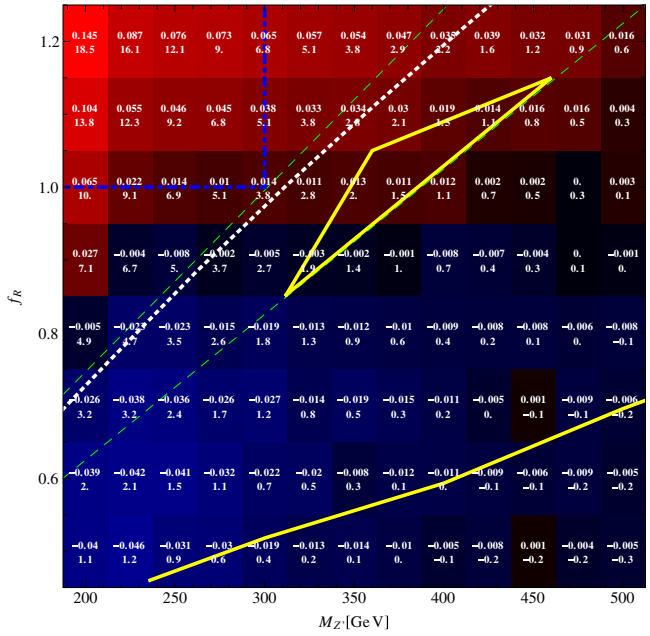

FIG. 4 (color online). t- and s-channel contributions to the charge asymmetry. In each cell, the upper number is the total NP contribution to the charge asymmetry, which should be between -0.037 and 0.023 to be consistent at a 95% C.L. with experiments [13] and theory [7]. The number below is the difference in units of the standard deviation of $\sigma_{t\bar{t}}^{\mathrm{SM+NP}}$ to the inclusive measured value of $\sigma_{t\bar{t}}$ at the LHC, as discussed in the text. The area delimited by the yellow (solid) triangle contains the region consistent with Tevatron limits in which these two observables differ by less than 2 standard deviations from the model predicted values. Tevatron limits are defined by the green (dashed) lines; APV excludes the region above the white (thick dotted) line. The blue (dot-dashed) line limits the region excluded by $tj/\bar{t}j$ resonance searches by CDF, while the region above the yellow (solid) line corresponds to the same searches by ATLAS. Since this last constraint would reject the allowed parameter space, we propose an increase in the Z' width to solve it. These constraints are discussed in Sec. IV.

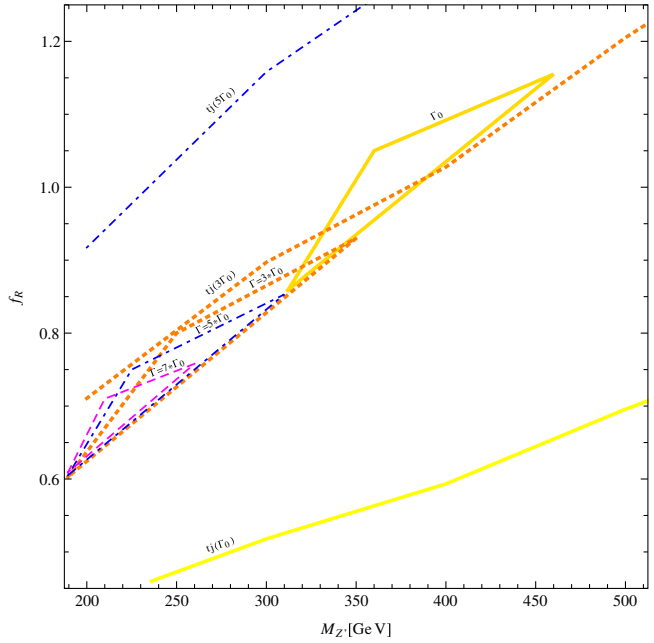

FIG. 5 (color online). The plotted triangles indicate the regions in parameter space compatible with all observables but the $tj/\bar{t}j$ resonance search, for different values of the Z' width. The yellow (solid) triangle corresponds to a Z' with its original width (Γ_0), when the decay is solely to u and $\bar{t}$. The orange (dotted), blue (dot-dashed), and magenta (dashed) triangles correspond to a Z' with its width increased by a factor of 3, 5, and 7, respectively. With the same style as for the allowed triangles, we plot the limit lines above which the parameter space is discarded due to $tj/\bar{t}j$ resonance search results. We find that increasing the original width by a factor of approximately 3 is enough to explain all observables.

When the Z' width is increased, the allowed areas of the parameter space appear displaced downward in Fig. 5, to smaller values of $M_{Z'}$ and f_R, relative to the yellow (solid) triangle. This can be understood by looking at Fig. 4. The numbers in the cells inside the triangle that correspond to the larger values of $M_{Z'}$ and f_R are those in which the predicted value for A_C is closer to the 95% C.L. allowed limit. These points are thus sensitive to getting excluded by any change in the model that could cause an increment in A_C. In fact, this is the case: When the Z' width becomes larger, the proportion of processes in the s-channel decreases, and, therefore, the negative contribution from A_{C_s} to A_C becomes smaller in absolute value. This translates into an increment of A_C that causes a deviation beyond the 95% C.L. in the upper region of the triangle. As a result, those points get excluded when the Z' width is increased.

With a similar argument, but this time concerning $\sigma_{t\bar{t}}$, it can be explained why parts of the excluded region in Fig. 4 become allowed in Fig. 5. In this case, the sensitive observable is $\sigma_{t\bar{t}}$, which decreases as the Z' width increases. The points inside the orange (dotted), blue (dot-dashed), and magenta (dashed) triangles in Fig. 5 are those where the difference of $\sigma_{t\bar{t}}$ to the measured value in units of the experimental error are larger than 2 in Fig. 4 and that is why they are excluded in this figure. However, they become allowed when the width is increased, since this makes $\sigma_{t\bar{t}}$ decrease.

Conclusively, in a given allowed region, in either Figs. 4 or 5, A_C is the most sensitive observable in the sector of large $M_{Z'}$ and f_R, and $\sigma_{t\bar{t}}$ in the sector of smaller $M_{Z'}$ and f_R.

Finally, we see that the triangles in Fig. 5 become smaller with larger values of the Z' width suggesting that it cannot be increased arbitrarily, because the effect of this increment on either A_C or $\sigma_{t\bar{t}}$ (or both) eventually becomes important enough so as to exclude most of the parameter space.

In the next section, we discuss the major constraints to the model, as well as its distinctive features.

IV. CONSTRAINTS AND PREDICTIONS OF THE MODEL

We have studied a model that simultaneously explains the apparently incompatible values of A_{FB} and A_C. In this section, we discuss the constraints to the model, its possible issues, and its distinctive features in the forecoming experimental results.

A. Direct constraint to the model

We study in the following paragraphs the direct constraint to the model coming from $tj/\bar{t}j$ resonance searches in $t\bar{t}j$ final states. Tevatron and LHC experiments have looked for this resonance as a possible explanation for the forward-backward asymmetry measurements at the Tevatron.

The first direct search for a particle X that would give a $tj/\bar{t}j$ resonance in $t\bar{t}j$ events was made by CDF in Ref. [44]. In this work they set upper limits at 95% C.L. on $t\bar{t}j$ production via the new resonance particle X, as a function of the resonance mass for couplings $g_L = 0$ and $g_R = 1$. Figure 4 shows the region of the parameter space excluded by this CDF search.

The CMS Collaboration also recently performed a search for a W' boson via the process $dg \to tW'$, $W' \to \bar{t}d$ [45]. The data showed no significant deviation from the standard model prediction and the W' model with $g_L = 0$ and $g_R = 2$ was excluded for a W' mass below 840 GeV in the combined ej and μj channels.

A recent work from ATLAS [46] also presents a search for a new W' produced in association with a $t/\bar{t}$ quark, leading to the resonance in question. They found the data to be consistent with the SM expectation and excluded a particle with mass below 350 GeV at 95% C.L, assuming unit right-handed coupling and null left-handed one. We have adapted their results to our model by assuming equal acceptance and adjusting the production cross section of the new particle and found relevant constraints to our model. In Fig. 4, we show that this experimental work discards the model if the Z' width is not modified. If the Z' width is increased, then the resonant $tj/\bar{t}j$ production cross section decreases. This yields that the model is allowed by all the studied observables if the width is greater than approximately 3 times its original value (see Fig. 5).

B. Indirect constraints to the model

Concerning the possible issues of the model, we have already mentioned its indirect constraints such as APV, $t\bar{t}j$, and single-top production. Let us analyze each of them in the following paragraphs.

As is well known, the model presented in this paper may come into conflict with APV observables. In Ref. [24] the limits given by APV have been studied in a model with a vector mediator coupled to u_R and t_R and a flavor-conserving boson. When we adapt their constraints to our model, we find the region compatible with APV limits for our model. These limits are given by the thick dotted line in Fig. 4 for a cutoff $\Lambda = 1000$ GeV. There are two main features of our model which, when contrasted to Ref. [24], relax the APV constraints. The first one is that in our model the Z' mass is larger than the top mass, and the second one is the fact that there is not a light flavor-conserving boson in our model. In any case, it is worth to mention at this point that the corrections to the calculation of the parity nonconservation in cesium are currently under discussion [35].

We have also already referred to the s-channel processes that contribute to the $t\bar{t}j$ production as a difficulty of the model. To overcome it, we have proposed an increment in the Z' width arguing that the new particle has invisible decays such as dark matter or sterile neutrinos. As there are not available works on $t\bar{t}j$ limits that could be adapted to our model, we have used $W'td$ production results from Ref. [43] as a rough estimation of the $t\bar{t}j$ production at the LHC in our model. We have checked that the $t\bar{t}j$ constraints in this work with 0.7 fb^{-1} would not exclude our model if the Z' width is increased by a factor of 3. We have also noted that the 5 fb^{-1} *projected* constraints would not affect the model if the increment of the width is of a factor of 5. Since d quark parton distribution functions are different from those of the u quarks, the analysis made in Ref. [43] cannot be adapted to our model straightforwardly and needs a new study.

The increment of the Z' width brings with it an excess in single-top production. Single-top quarks can be produced through three different processes in the SM: a t channel of the form $qb \to qt$ via the exchange of a W-like boson [47], a Wt associated production [48], and an s-channel process [49]. The t-channel process is dominant at both the LHC and the Tevatron. In our model, the single-top production topology is given by one reconstructed top and missing energy, with no extra b quark, different from that of the three processes mentioned. However, although the final state of the t-channel process and the Wt associated production at LO do not have missing energy, they are the only processes of the three that do not have an extra b quark. Henceforth, although the search strategy is not the same as that for the signature of our model, we may use these processes as a reference to know how unlikely could be the excess in single-top production predicted in our model. We use then, as an estimated reference, the latest measurements of the t channel and Wt associated single-top production. The ATLAS Collaboration results for both process cross sections summed yield $\sigma_t = 99.8 \pm 20.8$ pb [50,51], while those by CMS give $\sigma_t = 89.2 \pm 10.9$ pb [52,53]. In our model, for a Z' width increased by a factor of 3, the expected excess in the single-top production cross section is $\sim$(10–30) pb. In the case of the Z' width increased by a factor of 5 (7) this excess reaches $\sim$(10–40) [$\sim$(15–40)] pb.

The sum of the t channel and Wt associated single-top production cross section measured not only are in agreement with the predicted next-to-next-to-leading order sum of t and $\bar{t}$ cross sections for these processes, which is $\sigma_t = 80.2 \pm 2.1$ pb [47,48], but also with our predictions for an increased width in most of the parameter space at 95% C.L. The best agreement takes place when the Z' width is increased by a factor of 3.

In order to perform a precise study of the single-top production predicted in our model, one has to look for one reconstructed top, missing energy, and no extra b quark [54]. CDF [55] has reported a search of these characteristics, but for masses below those that we find favorable in this paper. A full search strategy for the single-top topology predicted in this model for the LHC is required [56].

At last, we should mention that, since the $t\bar{t}$ object is not created through the Z' in a resonant channel in any of the NP diagrams, the model should not be constrained by the usual $t\bar{t}$ resonance searches. Moreover, this model predicts a shape modification of the tail ($M_{t\bar{t}} \gtrsim 1$–1.5 TeV) of the spectrum, which is expected to be harder to measure than a resonant effect [57].

C. Distinctive features of the model

The most important distinctive feature of the model, and the cornerstone of this work, is the prediction of a large A_{FB} and a small or even negative A_C consistent with the experimental results from the Tevatron and the LHC in a region of the parameter space of the model.

Let us now investigate some other specific features of the model which could be exploited in order to test it. To do so, it is interesting to study cuts on the charge asymmetry.

A first cut is in the transverse momentum of the $t\bar{t}$ pair, $p_T(t\bar{t})$. As is well known, in the SM one expects A_C to grow with low p_T and vice versa [58]. In this model there is a particularity in the dependence of A_C with $p_T(t\bar{t})$ caused by the different s- and t-channel contributions to A_C that results in different contributions to the $p_T(t\bar{t})$. The s-channel processes involve a jet in the final state that provides the $t\bar{t}$ pair with an extra source of $p_T(t\bar{t})$ apart from that of the initial state radiation (ISR). This is not the case for the t-channel process, where the final state is $t\bar{t}$ and no additional sources of p_T other than ISR exists. As a result, one expects the s channel to be dominant for large values of $p_T(t\bar{t})$. Since the s channel contributes negatively to A_C, the model then predicts an excessive negative contribution to this observable when events with large $p_T(t\bar{t})$ are considered. On the contrary, for low values of $p_T(t\bar{t})$ the t channel is preferred, and one expects a smaller negative contribution from A_{C_s} to the charge asymmetry, i.e., an excess in the positive contributions to A_C coming from the t-channel processes. The first measurement of the dependence of A_C with $p_T(t\bar{t})$ for three bins in $p_T(t\bar{t})$ is presented in Ref. [13].

An observation concerning the simulation of events with ISR is that the ISR modeling in Monte Carlo simulations has large uncertainties. These uncertainties are large for A_C in the low $p_T(t\bar{t})$ region. On the contrary, for large enough values of this variable, the charge asymmetry becomes more independent of the ISR modeling, because the events passing such cuts in $p_T(t\bar{t})$ are dominated by gluon fusion events, which do not generate charge asymmetry. Only a tiny negative charge asymmetry is predicted by the few quark fusion events passing large cuts in $p_T(t\bar{t})$ [7,59]. Henceforth, the prediction of a negative excess in A_C for large values of $p_T(t\bar{t})$ is not affected by large ISR modeling uncertainties. This is a prediction of our model.

There is also another interesting cut on the charge asymmetry that could improve a NP search strategy. In this model the key channel is the s channel, which involves a qg collision and a $t\bar{t}j$ final state. In this kind of processes, due to the presence of the jet, the $t\bar{t}$ pair is likely to have an extra source of p_T apart from the already important contribution from initial state radiation of the incoming gluon. On the other hand, the incoming quark is likely to have considerably more momentum than the gluon so that the qg events are more likely to be boosted in the z direction, which translates into the $t\bar{t}$ pair having a large p_z as well. As a result, one could improve the search strategy, in virtue of the proton PDFs, by requesting the $t\bar{t}$ pair not only to have large p_T but also large p_z simultaneously.

There are other variables that can contribute to the discovery of NP models at the LHC similar to the model studied in this work. For instance, Ref. [34] investigates models where new X mediators generate a charge-asymmetric signal in tX production leading to observable new charge-asymmetric variables in $t\bar{t}j$ events. Among these are A_C as a function of the invariant mass and the transverse mass of various final state objects.

V. CONCLUSIONS

We have studied a phenomenological model with a new colorless, flavor-violating, electrically neutral Z' boson with right-handed couplings to u and t quarks. We assume that the Z' is charged so that it is not the same as its conjugate partner. We also consider that this particle mass is larger than the top mass.

The interaction term $\bar{u}tZ'$ and its Hermitian conjugate with $Z' \neq Z'^{\dagger}$ introduce three new processes at LO: one in which the new particle is exchanged through a t channel and the other two where it goes via an s channel. We have observed that the t-channel process contributes positively to both A_{FB} and A_C, and it is privileged at the Tevatron while the dominant s-channel one has a negative contribution and is turned on and only noticeable at the LHC, causing a cancellation of A_C measured by this accelerator. This cancellation is not present at the Tevatron, where actually a large A_{FB} has been measured. We have studied the dynamics of the two processes involved in the

cancellation in order to understand the mechanism through which it arises. This model then predicts a large positive A_{FB} and a null or even negative A_C.

We have studied the Tevatron and LHC phenomenology of this model and searched numerically for the cancellation mentioned. We investigated the allowed parameter space of the model by confronting it with several relevant and most stringent unfolded results from CDF and CMS at 95% C.L. and with its major constraints such as $tj/\bar{t}j$ resonance searches, atomic parity violation, and $t\bar{t}j$ and single-top production.

We found that constraints coming from atomic parity violation are not in conflict with our model. On the other hand, we found that existing results on $tj/\bar{t}j$ resonance searches and rough estimates of the $t\bar{t}j$ production cross section would discard the model unless the Z' width is increased. This assumes that the Z' decays to not detectable particles, such as dark matter or sterile neutrinos, a fraction of the times. We found that if the width is increased from its original value by a factor greater than 3, then the model can explain all studied observables. We show that this increment of the Z' width predicts single-top production with a particular topology not present in the SM single-top production: one reconstructed top and missing energy, with no extra b quark. As a result, in order to know how unlikely could be the excess in single-top production predicted in our model, we have used as a reference the two processes through which single tops are produced at LO in the SM that do not have a b quark in the final state. We found the excess to be consistent with our predictions for an increased width in most of the parameter space at 95% C.L. The best agreement takes place when the Z' width is increased by a factor of 3. Let us mention that $t\bar{t}u$ constraints and single-top search strategy studies are in progress. We expect that constraints coming from new results on the $t\bar{t}j$ cross section will be those that place the tightest limits on our model.

At last, we have presented some distinctive features of the model by studying cuts to the charge asymmetry. We have noted that in this model the dependence of A_C with $p_T(t\bar{t})$ is caused by the different s- and t-channel contributions to A_C which give rise to different contributions to the $p_T(t\bar{t})$. This results in a prediction of an excessive negative contribution to A_C when events with large $p_T(t\bar{t})$ are considered and, on the contrary, an excess in the positive contributions to A_C for low values of $p_T(t\bar{t})$. We expect a study in the large $p_T(t\bar{t})$ region to be more Monte Carlo independent than a study in the low $p_T(t\bar{t})$ region. We finally found that, because of the PDFs, one could improve the search strategy by requesting the $t\bar{t}$ pair to have not only large p_T but also, simultaneously, large p_z.

We have shown that our model brings compatibility to the apparent disagreement between $t\bar{t}$ Tevatron forward-backward asymmetry and LHC charge asymmetry. Let us finally remark that all the analysis has been made confronting our model with the Tevatron and LHC experimental results that seem to be more incompatible. If results with a smaller apparent discrepancy were to be used, the constraints to the Z' model would be less restrictive.

ACKNOWLEDGMENTS

We thank J. Adelman and M. Peskin for useful discussions. E. A. thanks SLAC, where part of this work was carried out.

Note added.—The results found in this paper were first presented in July 2012 at ICHEP2012 [27] and then submitted to the arXiv [60] in September. The day after appearing in the arXiv, a work [61] with mostly the same results was also submitted to the arXiv.

[1] G. Aad *et al.* (ATLAS Collaboration), arXiv:1207.7214.
[2] S. Chatrchyan *et al.* (CMS Collaboration), arXiv:1207.7235.
[3] C. T. Hill and S. J. Parke, Phys. Rev. D **49**, 4454 (1994); C. T. Hill and E. H. Simmons, Phys. Rep. **381**, 235 (2003); K. Agashe, R. Contino, and R. Sundrum, Phys. Rev. Lett. **95**, 171804 (2005).
[4] T. Aaltonen *et al.* (CDF Collaboration), Phys. Rev. D **83**, 112003 (2011).
[5] CDF Collaboration, Report No. 10807, http://www-cdf.fnal.gov/physics/new/top/2012/LepJet_AFB_Winter2012/CDF10807.pdf; A. Lister (CDF and D0 Collaborations), arXiv:0810.3350; T. Aaltonen *et al.* (CDF Collaboration), Phys. Rev. Lett. **101**, 202001 (2008); V. M. Abazov *et al.* (D0 Collaboration), Phys. Rev. D **84**, 112005 (2011).
[6] E. Shabalina *et al.* (CDF and D0 Collaborations), Eur. Phys. J. Web Conf. **28**, 05003 (2012).
[7] J. H. Kuhn and G. Rodrigo, J. High Energy Phys. 01 (2012) 063.
[8] T. Aaltonen *et al.* (CDF Collaboration), Phys. Rev. Lett. **101**, 202001 (2008).
[9] CDF Collaboration, Report No. 10807, http://www-cdf.fnal.gov/physics/new/top/2012/LepJet_AFB_Winter2012/CDF10807.pdf.
[10] V. M. Abazov *et al.* (D0 Collaboration), Phys. Rev. D **84**, 112005 (2011).
[11] P. Ferrario and G. Rodrigo, Phys. Rev. D **80**, 051701 (2009); A. Djouadi, G. Moreau, F. Richard, and R. K. Singh, Phys. Rev. D **82**, 071702 (2010); S. Jung, H. Murayama, A. Pierce, and J. D. Wells, Phys. Rev. D **81**, 015004 (2010); Q.-H. Cao, D. McKeen, J. L. Rosner, G. Shaughnessy, and C. E. M. Wagner, Phys. Rev. D **81**, 114004 (2010); J. A. Aguilar-Saavedra, Nucl. Phys. **B843**, 638 (2011); L. Da Rold, J. High Energy Phys. 02

(**2011**) 034; G. Burdman, L. de Lima, and R. D. Matheus, Phys. Rev. D **83**, 035012 (2011); B. Xiao, Y.-k. Wang, and S.-h. Zhu, arXiv:1011.0152; E. Alvarez, L. Da Rold, and A. Szynkman, J. High Energy Phys. 05 (2011) 070; Y. Bai, J. L. Hewett, J. Kaplan, and T. G. Rizzo, J. High Energy Phys. 03 (2011) 003; V. Barger, W.-Y. Keung, and C.-T. Yu, Phys. Lett. B **698**, 243 (2011); Z. Ligeti, M. Schmaltz, and G. M. Tavares, J. High Energy Phys. 06 (2011) 109; J. A. Aguilar-Saavedra and M. Perez-Victoria, J. High Energy Phys. 05 (2011) 034; N. Craig, C. Kilic, and M. J. Strassler, Phys. Rev. D **84**, 035012 (2011); C. Degrande, J.-M. Gerard, C. Grojean, F. Maltoni, and G. Servant, Phys. Lett. B **703**, 306 (2011); J. A. Aguilar-Saavedra and M. Perez-Victoria, Phys. Lett. B **701**, 93 (2011); Phys. Rev. D **84**, 115013 (2011); R. Barcelo, A. Carmona, M. Masip, and J. Santiago, Phys. Lett. B **707**, 88 (2012); R. Barcelo, A. Carmona, M. Chala, M. Masip, and J. Santiago, Nucl. Phys. **B857**, 172 (2012); E. Alvarez, L. Da Rold, J. I. S. Vietto, and A. Szynkman, J. High Energy Phys. 09 (2011) 007; J. A. Aguilar-Saavedra, Nuovo Cimento Soc. Ital. Fis. C **035N3**, 167 (2012); J. A. Aguilar-Saavedra and A. Juste, Phys. Rev. Lett. **109**, 211804 (2012); M. Cvetič, J. Halverson, and P. Langacker, J. High Energy Phys. 11 (2012) 064, among *many* others.

[12] ATLAS Collaboration, Report No. ATLAS-CONF-2012-057, 2012.

[13] S. Chatrchyan *et al.* (CMS Collaboration), Phys. Lett. B **717**, 129 (2012).

[14] G. Aad *et al.* (ATLAS Collaboration), Phys. Lett. B **708**, 37 (2012).

[15] G. Aad *et al.* (ATLAS Collaboration), New J. Phys. **13**, 053044 (2011).

[16] S. Jung, H. Murayama, A. Pierce, and J. D. Wells, Phys. Rev. D **81**, 015004 (2010).

[17] Q.-H. Cao, D. McKeen, J. L. Rosner, G. Shaughnessy, and C. E. M. Wagner, Phys. Rev. D **81**, 114004 (2010).

[18] V. Barger, W.-Y. Keung, and C.-T. Yu, Phys. Lett. B **698**, 243 (2011).

[19] J. Shu, K. Wang, and G. Zhu, Phys. Rev. D **85**, 034008 (2012).

[20] E. L. Berger, Q.-H. Cao, C.-R. Chen, C. S. Li, and H. Zhang, Phys. Rev. Lett. **106**, 201801 (2011).

[21] E. L. Berger, arXiv:1109.3202.

[22] S. Y. Ayazi, arXiv:1207.0643.

[23] P. Ko, Y. Omura, and C. Yu, arXiv:1208.4675.

[24] M. I. Gresham, I.-W. Kim, S. Tulin, and K. M. Zurek, Phys. Rev. D **86**, 034029 (2012).

[25] K. Cheung and T.-C. Yuan, Phys. Rev. D **83**, 074006 (2011); K. Cheung, W.-Y. Keung, and T.-C. Yuan, Phys. Lett. B **682**, 287 (2009).

[26] S. Jung, A. Pierce, and J. D. Wells, Phys. Rev. D **83**, 114039 (2011).

[27] E. C. Leskow and E. Álvarez, Proc. Sci., ICHEP2012 (2012) 201.

[28] G. Zhu, Phys. Lett. B **703**, 142 (2011).

[29] M. Duraisamy, A. Rashed, and A. Datta, Phys. Rev. D **84**, 054018 (2011).

[30] S. Chatrchyan *et al.* (CMS Collaboration), arXiv:1208.0957.

[31] S. Chatrchyan *et al.* (CMS Collaboration), J. High Energy Phys. 08 (2012) 110.

[32] M. I. Gresham, I.-W. Kim, and K. M. Zurek, Phys. Rev. D **84**, 034025 (2011).

[33] Y. Cui, Z. Han, and M. D. Schwartz, J. High Energy Phys. 07 (2011) 127.

[34] S. Knapen, Y. Zhao, and M. J. Strassler, Phys. Rev. D **86**, 014013 (2012).

[35] V. A. Dzuba, J. C. Berengut, V. V. Flambaum, and B. Roberts, Phys. Rev. Lett. **109**, 203003 (2012); V. A. Dzuba and V. V. Flambaum, Int. J. Mod. Phys. E **21**, 1230010 (2012).

[36] C. S. Wood, S. C. Bennett, D. Cho, B. P. Masterson, J. L. Roberts, C. E. Tanner, and C. E. Wieman, Science **275**, 1759 (1997); J. Gúena, M. Lintz, and M. A. Bouchiat, Phys. Rev. A **71**, 042108 (2005).

[37] F. Maltoni and T. Stelzer, J. High Energy Phys. 02 (2003) 027.

[38] E. Alvarez, L. Da Rold, and A. Szynkman, J. High Energy Phys. 05 (2011) 070.

[39] T. Aaltonen *et al.* (CDF Collaboration), Report No. 9913, 2009.

[40] CMS Collaboration, Report No. CMS-PAS-TOP-11-024.

[41] M. Aliev, H. Lacker, U. Langenfeld, S. Moch, P. Uwer, and M. Wiedermann, Comput. Phys. Commun. **182**, 1034 (2011).

[42] J. Alwall *et al.*, Eur. Phys. J. C **53**, 473 (2008).

[43] D. Duffty, Z. Sullivan, and H. Zhang, Phys. Rev. D **85**, 094027 (2012).

[44] T. Aaltonen *et al.* (CDF Collaboration), Phys. Rev. Lett. **108**, 211805 (2012).

[45] S. Chatrchyan *et al.* (CMS Collaboration), Phys. Lett. B **717**, 351 (2012).

[46] ATLAS Collaboration, Report No. ATLAS-CONF-2012-096, 2012.

[47] N. Kidonakis, Phys. Rev. D **83**, 091503 (2011).

[48] N. Kidonakis, Phys. Rev. D **82**, 054018 (2010).

[49] N. Kidonakis, Phys. Rev. D **81**, 054028 (2010).

[50] G. Aad *et al.* (ATLAS Collaboration), Phys. Lett. B **717**, 330 (2012).

[51] G. Aad *et al.* (ATLAS Collaboration), Phys. Lett. B **716**, 142 (2012).

[52] S. Chatrchyan *et al.* (CMS Collaboration), arXiv:1209.4533.

[53] J. O. o. b. o. t. C. Collaboration (CMS Collaboration), Eur. Phys. J. Web Conf. **28**, 12041 (2012).

[54] J. Andrea, B. Fuks, and F. Maltoni, Phys. Rev. D **84**, 074025 (2011); H. Davoudiasl, D. E. Morrissey, K. Sigurdson, and S. Tulin, Phys. Rev. D **84**, 096008 (2011); E. L. Berger, B. W. Harris, and Z. Sullivan, Phys. Rev. Lett. **83**, 4472 (1999); Phys. Rev. D **63**, 115001 (2001).

[55] T. Aaltonen *et al.* (CDF Collaboration), Phys. Rev. Lett. **108**, 201802 (2012).

[56] E. Alvarez and E. C. Leskow (work in progress).

[57] C. Degrande, J.-M. Gerard, C. Grojean, F. Maltoni, and G. Servant, J. High Energy Phys. 03 (2011) 125.

[58] E. Alvarez, Phys. Rev. D **85**, 094026 (2012); **86**, 037501 (2012).

[59] P. Skands, B. Webber, and J. Winter, J. High Energy Phys. 07 (2012) 151.

[60] E. Alvarez and E. C. Leskow, arXiv:1209.4354.

[61] J. Drobnak, A. L. Kagan, J. F. Kamenik, G. Perez, and J. Zupan, Phys. Rev. D **86**, 094040 (2012).